

# Strength and microstructure of diatomaceous earth-based geopolymer paste: Optimization of molarity and alkali activator proportion

Munirul Hady<sup>1,2</sup>, Taufiq Saidi<sup>2\*</sup>, Muttaqin Hasan<sup>2</sup>, Sugiarto<sup>2</sup>

<sup>1</sup> Doctoral Program, School of Engineering, Post Graduate Program, Universitas Syiah Kuala, Banda Aceh, 23111, Indonesia

<sup>2</sup> Department of Civil Engineering, Universitas Syiah Kuala, Banda Aceh, 23111, Indonesia

\* Corresponding author's e-mail: [taufiq\\_saidi@usk.ac.id](mailto:taufiq_saidi@usk.ac.id)

## ABSTRACT

This research focused on refining alkali activator parameters to enhance the mechanical performance and microstructural characteristics of diatomaceous earth (DE) based geopolymer paste. The influence of sodium hydroxide (NaOH) concentration (10, 12, and 14 M) and the sodium silicate to sodium hydroxide ratio ( $\text{Na}_2\text{SiO}_3/\text{NaOH}$ ) (0.5, 1.0, and 2.0) on key response variables was evaluated using response surface methodology (RSM), including compressive strength, flexural strength, flowability, and initial setting time. The optimal mixture was identified at a NaOH concentration of 10 M and a sodium silicate proportion of 53.04% in the total activator solution, resulting in a compressive strength of 18.05 MPa and a flexural strength of 2.32 MPa. Microstructural investigations using SEM–EDS, XRD, and FTIR confirmed the formation of a compact geopolymer matrix with low porosity, predominantly composed of sodium aluminosilicate hydrate (N–A–S–H) gel. ANOVA results indicated that the  $\text{Na}_2\text{SiO}_3$  to total activator ratio had a more significant effect on mechanical properties ( $p < 0.05$ ) than NaOH molarity. Furthermore, the empirical model demonstrated strong predictive reliability, with deviations between predicted and experimental values remaining below 5%. The minimal errors in flow (0.74%) and initial setting time (1.51%) reflect accurate prediction of fresh state behavior and reaction kinetics, while the low errors in compressive (2.95%) and flexural strength (4.04%) confirm the model's capability to estimate hardened state performance. Overall, the optimized alkali activation regime significantly improved the geopolymerization of DE, supporting its potential as a sustainable, locally sourced construction material with enhanced performance. This study presents a novel approach by simultaneously optimizing NaOH molarity and  $\text{Na}_2\text{SiO}_3/\text{NaOH}$  ratio using response surface methodology (RSM) to enhance both mechanical performance and microstructural characteristics of diatomaceous earth-based geopolymer paste, providing a comprehensive optimization framework not previously reported.

**Keywords:** geopolymer, diatomaceous earth, NaOH molarity, microstructure, alkali activator proportion, strength.

## INTRODUCTION

The search for natural alternatives is being driven by increasingly complex environmental problems, such as water pollution by heavy metals, industrial waste, and the high demand for sustainable and environmentally friendly functional materials. One material gaining attention is diatomaceous earth (DE) [1], which is particularly relevant as Portland cement production contributes 8% of global  $\text{CO}_2$  emissions, and

promotes the search for alternative materials such as geopolymer [2]. DE based geopolymer has high potential due to elevated amorphous silica content (>80%) and abundant availability [3].

DE is a siliceous sediment formed from the accumulation of fossilized shell (frustules) of diatoms, a single celled algae that has lived in fresh and seawater for several years. The unique, porous shell structure, very high surface area, and chemical composition dominated by amorphous silica ( $\text{SiO}_2 \cdot n\text{H}_2\text{O}$ ) make DE a material with excellent

adsorption properties, mild abrasiveness, thermal insulation, and permeability[4]. It is also relatively abundant in nature and can be mined economically, as the inert, non toxic, and natural origin shows high compatibility with the principles of green technology [5]. However, the application has been limited to traditional use, such as filter media, particularly in the beer and wine filtration industry, including mild abrasives in toothpaste, liquid spill absorbents, and natural insecticides[6].

Slight modifications of DE through physical or chemical such as calcination, acid activation, or surface functionalization, have been shown to improve performance significantly. Several studies have shown that modified DE is an effective adsorbent for the adsorption of heavy metal ions, including Pb, Cd, and Cu, organic dyes from textile wastewater, and pharmaceutical compounds in water [7]. Furthermore, in the field of advanced materials, it has potential as a catalyst support, a material for making porous ceramics, a polymer composite material for increasing mechanical strength, and an anode in lithium ion batteries[8]. The experiment from [9] confirmed Geopolymer composites have emerged as sustainable structural materials offering high strength to weight ratios, improved durability, and reduced environmental impact compared with conventional cementitious and metallic systems. Understanding their static, vibration, and buckling behavior is essential for reliable structural design, for which classical lamination theory provides an effective analytical framework. Several studies have also documented the utilization of calcined DE as a partial substitute for cement [10–15]. However, the use of DE as a base material for geopolymer is still very rare. This shows the need for further investigations to optimize the modification process and explore new, more innovative, as well as high value added applications, including geopolymer. The performance of DE is highly dependent on the parameters of alkali activator (NaOH and Na<sub>2</sub>SiO<sub>3</sub>), particularly NaOH molarity and Na<sub>2</sub>SiO<sub>3</sub>/NaOH ratio, which control silica dissolution and the formation of N-A-S-H matrix [16]. Madirisha et al. [11] reported that geopolymer paste activated with alkali aluminosilicate (AAS) or aluminosilicate phosphate (ASP) could be a sustainable construction material with a low carbon footprint. The mechanical properties and durability were found to be highly influenced by the chemical profile of the precursor substance, molar ratio, type of hardener (NaOH or phosphoric acid), and curing process.

Previous studies on similar materials, namely fly ash and metakaolin, showed the dependence of compressive strength on the molarity range of 8–16 M and ratio of 1.0–2.5 [17]. Another report [18] on DE based geopolymer with 10 M NaOH and ratio of 1.5, only achieved a compressive strength of 18 MPa, which showed the potential for improvement through systematic optimization. Therefore, this study is expected to optimize NaOH molarity (10–14 M) and Na<sub>2</sub>SiO<sub>3</sub>/NaOH ratio (0.5–2.5) to maximize compressive strength and analyze the correlation between activator parameters, mechanical performance, and microstructural changes. A study by Enoh and Ushie [14] showed that Na<sub>2</sub>SiO<sub>3</sub>/NaOH ratio of 1.0 and NaOH concentration of 10 M produced an optimal compressive strength of 14.6 MPa in metakaolin based geopolymer binders, while a ratio above 1.0 actually decreased the strength. Abdullah et al. [15] stated that in the geopolymerization process, a NaOH concentration of 12 M produced the best impact strength on fly ash geopolymer aggregates. Meanwhile, lower (6 M) or higher (14 M) concentrations produced reduced strength due to a lack of dissolution or excess Na<sup>+</sup> and OH<sup>-</sup> ions interfering with matrix formation.

Several reports have shown high strength at moderate concentrations, but decreased strength at excessively elevated molarities. The majority of previous studies also used a trial and error method, which was less efficient in identifying the best combination of factors. To address this inefficiency, the use of modern statistical methods such as Response Surface Methodology (RSM) has proven effective in optimizing variables with minimal experimentation, although there is limited application to DE based geopolymer [19]. Therefore, this study aims to obtain the optimal combination of the NaOH molarity and the ratio between Na<sub>2</sub>SiO<sub>3</sub> and NaOH in the manufacture of DE based geopolymer using RSM analysis by maximizing mechanical properties, including compressive and flexural strength. Rheological properties are also evaluated, including flow and initial setting time, as well as the microstructure of geopolymer [20]. The experiment uses a factorial design with three levels of NaOH molarity and Na<sub>2</sub>SiO<sub>3</sub>/NaOH ratio. The results are expected to provide a scientific basis for using DE as a sustainable geopolymer precursor, while contributing to reducing dependence on cement and suppressing CO<sub>2</sub> emissions from the construction sector. The novelty of this study lies in the use

of only DE as a precursor for geopolymer, which has not been previously reported. Moreover, this study presents a novel approach by simultaneously optimizing NaOH molarity and  $\text{Na}_2\text{SiO}_3/\text{NaOH}$  ratio using RSM to enhance both mechanical performance and microstructural characteristics of DE-based geopolymer.

## MATERIALS AND METHODS

### Materials

The materials employed in this study consisted of diatomaceous earth (DE), an alkali activator solution, water, and a superplasticizer. The activator system comprised two components sodium hydroxide (NaOH) and sodium silicate ( $\text{Na}_2\text{SiO}_3$ ) prepared using laboratory grade clean water. A polycarboxylate based superplasticizer with a specific gravity of 1.06 was incorporated to improve workability. The DE was sourced from Lambeurenut Village in Aceh Besar Regency, then ground and sieved through a #200 mesh. The resulting powder was oven dried at 100 °C for 24 hours and subsequently calcined at 700 °C for 5 hours in a laboratory furnace, as illustrated in Figure 1. The calcined DE possessed a density of 770  $\text{kg}/\text{m}^3$ , an SSD specific gravity of 2.00, an oven dry specific gravity of 1.89, and a water absorption capacity of 6.54%.

The chemical constituents of the DE was determined through X-ray fluorescence (XRF) analysis performed with a Rigaku Supermini 200 analyzer. As summarized in Table 1, the major oxides present were  $\text{SiO}_2$  (44%), CaO (12.9%),  $\text{Al}_2\text{O}_3$  (8.46%), and  $\text{Fe}_2\text{O}_3$  (3.89%). Although the

$\text{SiO}_2$  content was relatively moderate, the elevated CaO proportion suggests favorable reactivity when incorporated into cementitious and geopolymer systems. In addition, the particle size distribution of the DE was evaluated using a particle size analyzer (PSA), specifically the MicroBrook 2000 L. The results shown in Figure 2 indicate a predominance of fine particles in the micrometer range, which contributes to a high specific surface area and enhances its potential effectiveness for adsorption as well as its role as a filler in cement mortar and geopolymer applications.

Surface and morphological analyses of DE before and after calcination were conducted using a Hitachi SU-3500 scanning electron microscope, results presented in Figures 3 and 4. The morphology before and after milling and calcination showed a cellular structure with numerous nanopores distributed on the surface. However, before calcination, there were hollow and irregular pores, whose structure appeared cleaner and denser after calcination due to the removal of organic and volatile components. This was similar to previous studies [21, 22] where heat treatment causes a more regular pore structure and increased adsorption capacity.

Analysis of the mineral characteristics and crystal structure of DE was carried out using a Shimadzu maxima XRD tester. As shown in Figure 5, DE structure was dominated by amorphous silica phase with the presence of additional minerals such as quartz and calcite. Furthermore, there was silica in crystalline form, namely quartz.

Flowchart of this experiment as shown in Figure 6 illustrating the systematic experimental methodology of the study, including material preparation, geopolymer mixture design,

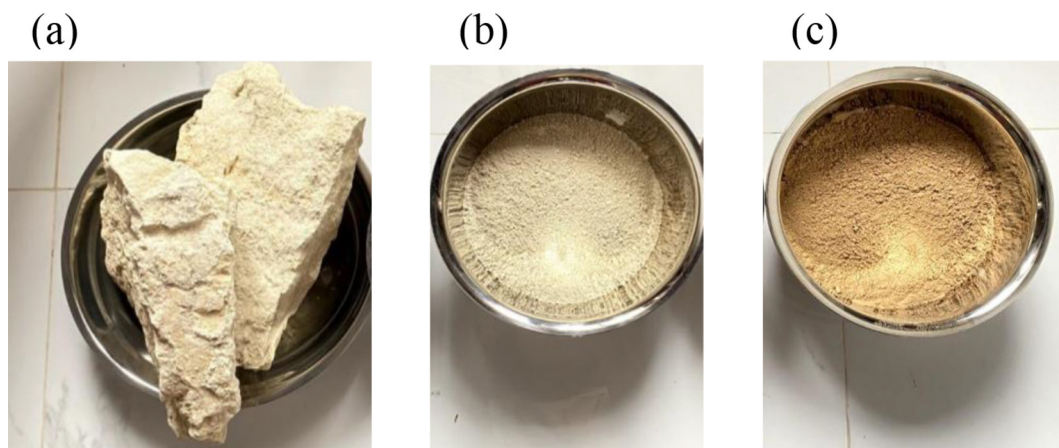


Figure 1. Process of DE raw material (a) Block of DE (b) Grinded DE (c) Calcined DE

**Table 1.** Chemical composition of DE

Chemical substance	Percentage (%)
MgO	0.685
Al <sub>2</sub> O <sub>3</sub>	8.46
SiO <sub>2</sub>	44.0
P <sub>2</sub> O <sub>5</sub>	0.0759
SO <sub>3</sub>	0.106
Cl	0.527
K <sub>2</sub> O	1.29
CaO	12.9
TiO <sub>2</sub>	0.539
MnO	0.0292
Fe <sub>2</sub> O <sub>3</sub>	3.89
NiO	0.0113
ZnO	0.0121
Rb <sub>2</sub> O	0.0063
SrO	0.0434
ZrO <sub>2</sub>	0.0170
Balance	27.4

laboratory testing, statistical optimization using RSM and ANOVA, experimental validation, and microstructural analysis of the optimized diatomaceous earth-based geopolymer paste.

### Experimental design

In this study, an alternative material used was diatomaceous earth. Previous research has shown that the principal component of DE is amorphous silica, with levels reaching around 55–70%, depending on the local environment. The silica

compound content in diatomaceous earth varies greatly, which is influenced by the region of origin of the material [23]. The experiment used a factorial design with two factors, namely NaOH molarity and Na<sub>2</sub>SiO<sub>3</sub>/NaOH ratio. Each factor had three levels, leading to 9 mixture proportions as shown in Table 2. NaOH molarity levels were set at 10, 12, and 14 M, while Na<sub>2</sub>SiO<sub>3</sub>/NaOH ratio levels were at 1:1, 2:1, and 1:2 based on the weight ratio. To facilitate the analysis, the factor was changed to Na<sub>2</sub>SiO<sub>3</sub>/total activator ratio and expressed as a percentage, rather than using Na<sub>2</sub>SiO<sub>3</sub>/NaOH ratio. Na<sub>2</sub>SiO<sub>3</sub>/total activator ratio for each Na<sub>2</sub>SiO<sub>3</sub>/NaOH ratio is shown in Table 2. Based on weight ratio of the activator solution to DE of 0.6, the amount of DE used for all mixtures was the same. Similarly, the weight of water and superplasticizer used in each mixture was the same, namely 15% and 2% of the weight of DE, respectively.

### Geopolymer mixture proportion and specimen preparation

To achieve the targeted molarities, solid NaOH was dissolved in distilled water to prepare solutions with concentrations of 10, 12, and 14 M. The NaOH solution was then blended with Na<sub>2</sub>SiO<sub>3</sub> according to the proportions specified in Table 2. Subsequently, diatomaceous earth, additional water, and the superplasticizer were incorporated and mixed thoroughly to obtain a uniform geopolymer paste. The fresh paste was evaluated for flow and initial setting time using a flow table and Vicat apparatus in accordance with ASTM C1437 and ASTM C191, respectively [24, 25]. For the flow

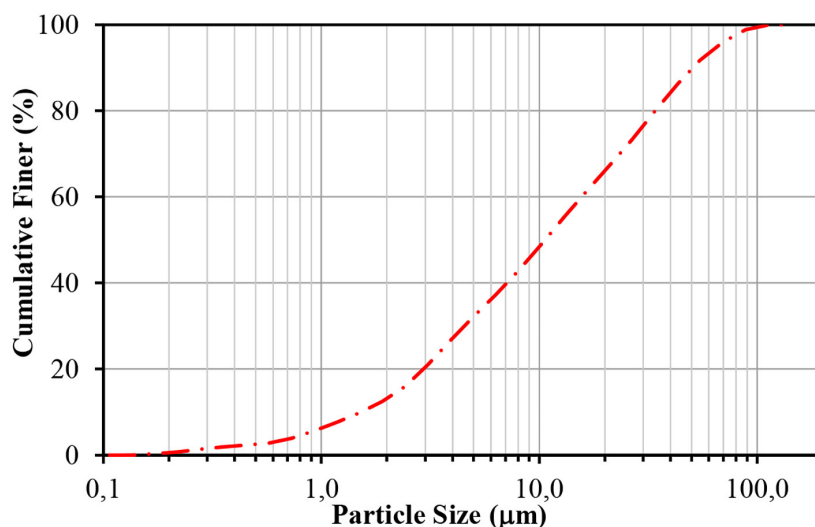


**Figure 2.** Particle size distribution for diatomite earth

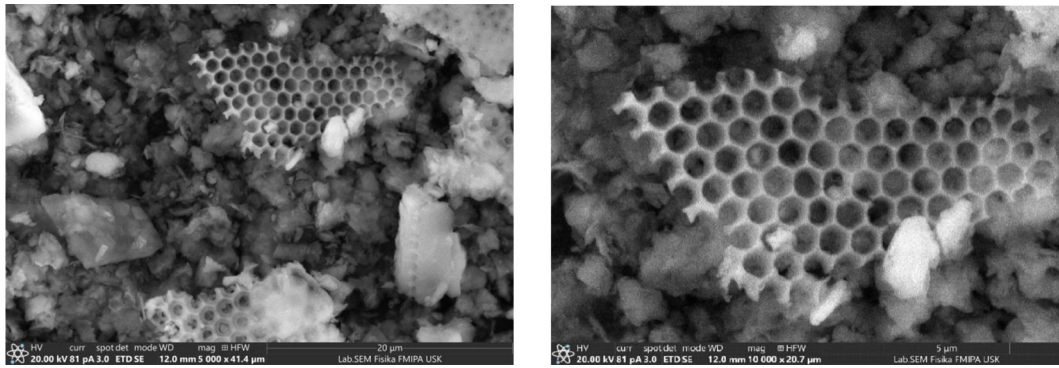


Figure 3. SEM microphotograph of DE before calcination

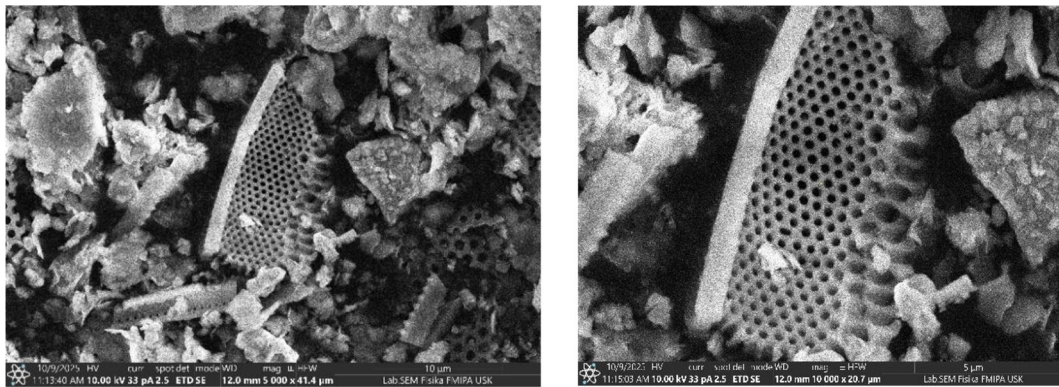


Figure 4. SEM microphotograph of DE after calcination

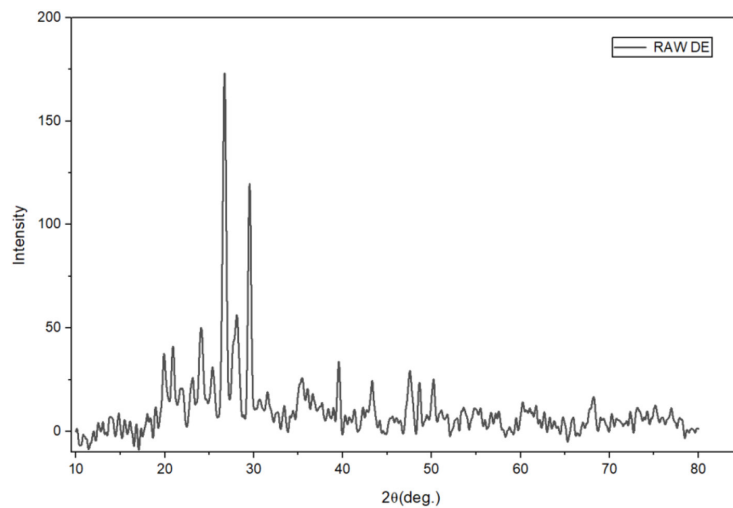


Figure 5. XRD patterns of DE

test, the fresh mixture was placed into a standard cone mold on the flow table, the mold was carefully lifted, and the sample was compacted 25 times. The resulting spread was measured and expressed as a percentage of flow, reflecting the workability and plasticity of the mixture. The initial setting time was then determined by placing the paste in a Vicat

mold and observing the penetration of the needle at regular intervals. The initial set was recorded when the needle no longer reached the base, while the final setting time was identified when the needle left only a slight impression on the surface, providing an indication of the early reaction and stiffening behavior of the geopolymer paste.

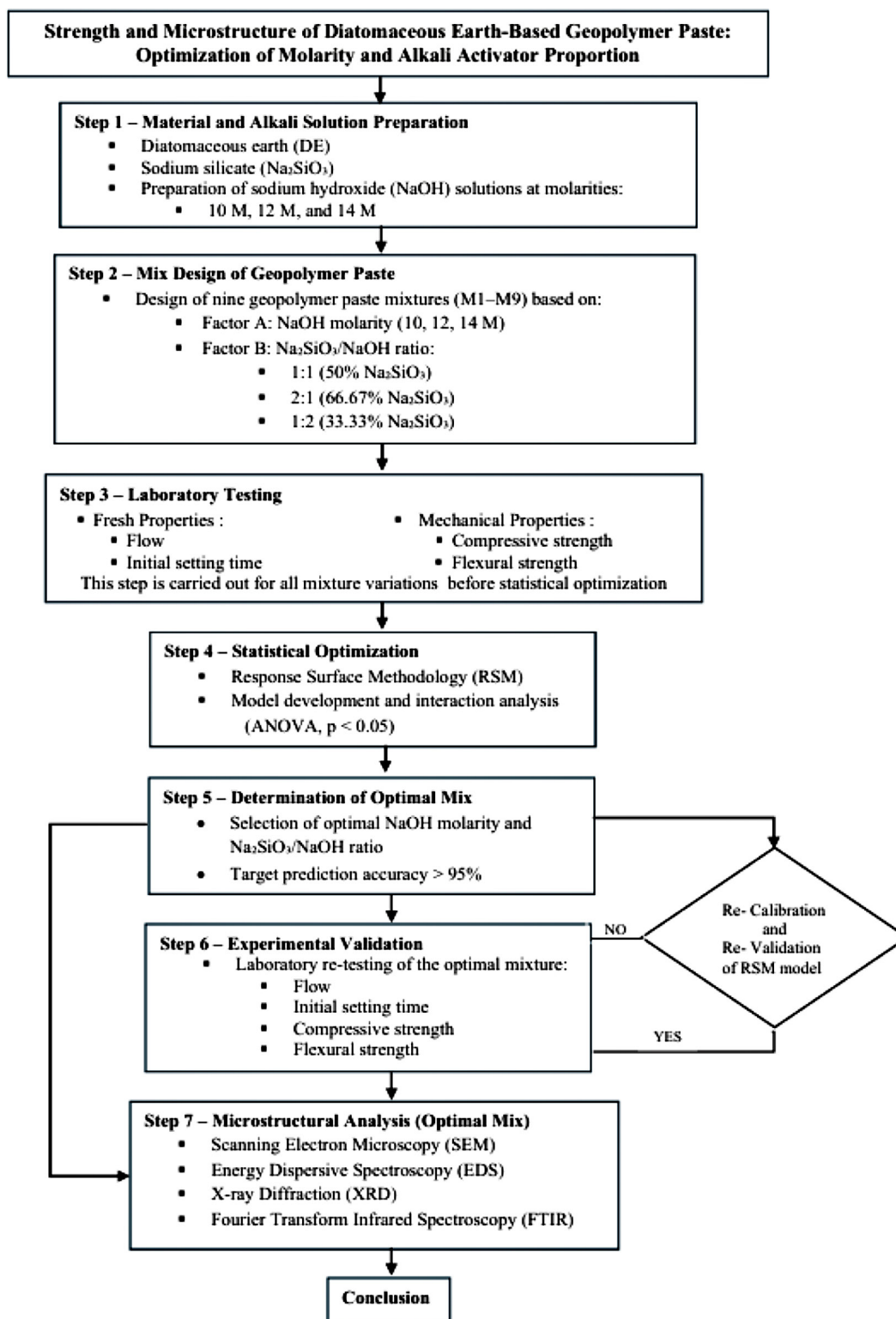


Figure 6. Experimental flowchart for diatomaceous earth based geopolymer paste

The geopolymer specimens were fabricated by casting the fresh paste into prepared molds. Specimens in cube form (50 × 50 × 50 mm) were used to determine compressive strength, whereas beam shaped specimens (40 × 40 × 160 mm) were prepared to measure flexural strength. After

casting, all specimens were kept in the molds at room temperature for 24 hours, followed by oven curing at 90 °C for another 24 hours. The specimens were then demolded, sealed in airtight plastic bags, and stored under indoor conditions until the designated testing ages.

**Table 2.** Mixture proportion of geopolymer

Mixtures	Factor 1: NaOH Molarity	Factor 2: Activator ratio	
		Na <sub>2</sub> SiO <sub>3</sub> /NaOH	Na <sub>2</sub> SiO <sub>3</sub> /total activator (%)
M1	10	1:1	50
M2	12	1:1	50
M3	14	1:1	50
M4	10	2:1	66.67
M5	12	2:1	66.67
M6	14	2:1	66.67
M7	10	1:2	33.33
M8	12	1:2	33.33
M9	14	1:2	33.33

Compressive strength tests were performed on cube specimens at curing ages of 3, 7, and 28 days using a universal testing machine, following ASTM C109/109M [26] as shown in Figure 7(a). The compressive strength was determined by dividing the maximum applied load by the cross sectional area of the specimen. For the flexural strength test, beam specimens were placed on two supports with a span length of 100 mm and subjected to a central point load until failure, in accordance with ASTM C78/78M [27] as shown in Figure 7(b). The recorded maximum load was then used to calculate the corresponding flexural strength.

**RSM analysis**

Optimization of NaOH molarity and Na<sub>2</sub>SiO<sub>3</sub>/total activator ratio was analyzed using RSM by

enhancing all responses. These included compressive strength, flexural strength, flow rate, and initial setting time simultaneously, widely known as multi objective optimization. Since the quality of geopolymer increased alongside higher compressive and flexural strength values, the expected objectives of all compressive and flexural strength responses were to produce maximum values. Meanwhile, flow rate and initial setting time, as well as NaOH molarity and Na<sub>2</sub>SiO<sub>3</sub>/total activator ratio, should be in the experimental range. Table 3 presents the factors used in the optimization process and the desired response targets for this research. The application of response surface methodology (RSM) has been widely reported as an effective approach for developing empirical models that describe the relationship between process parameters and response variables in engineering studies [28]. The statistical validity and adequacy of these models are commonly evaluated using analysis of variance (ANOVA), which enables the identification of significant factors and interaction effects while ensuring the reliability of the regression models [29]. Furthermore, the integration of validated RSM models into a multi-objective optimization framework has been extensively adopted to simultaneously optimize multiple conflicting performance criteria and to obtain optimal trade-off solutions for practical engineering applications.

For RSM analysis in this study, a second order regression model was selected as given in Equation 1. The model suitability was tested using analysis of variance (ANOVA). When ANOVA results



**Figure 7.** (a) Compressive strength test and (b) Flexural strength test

**Table 3.** Desired objectives in multi objective optimization

Optimized items	Unit	Lower limit	Upper limit	Desired goal
NaOH molarity	M	10	14	In range
Na <sub>2</sub> SiO <sub>3</sub> /total activator	%	33.33	66.67	In range
Compressive strength	MPa	2.30	18.73	Maximum
Flexural strength	MPa	0.27	2.40	Maximum
Flow	%	5.41	27	In range
Initial setting time	minutes	30	270	In range

showed a p-value  $\leq 0.05$ , the selected model was considered significant. However, with p-value  $\geq 0.05$ , the selected model was not significant, showing the need for another regression model.

$$Y = \beta_0 + \beta_1A + \beta_2B + AB + \beta_4A^2 + \beta_5B^2 \quad (1)$$

where:  $Y$  – response variables,  $b_0$  – intercept term,  $b_1, b_2$  – first order terms,  $b_3$  – binary interaction terms,  $b_4, b_5$  – quadratic terms,  $A$  – NaOH molarity, and  $B$  – Na<sub>2</sub>SiO<sub>3</sub>/total activator ratio. RSM analysis in this study uses Design Expert software.

#### Model validation and microstructure analysis

To verify the reliability of the RSM derived model, an additional geopolymer mixture was produced using the optimal values of NaOH molarity and Na<sub>2</sub>SiO<sub>3</sub> to total activator ratio obtained from the multi objective optimization results. This mixture was then evaluated in terms of flow behavior, initial setting time, compressive strength, and flexural strength. The experimental outcomes were subsequently compared with the values predicted by the second order regression model to assess its accuracy. In parallel, the microstructural characteristics of the optimized DE based geopolymer were examined using fourier transform infrared spectroscopy (FTIR), scanning electron microscopy coupled with energy dispersive spectroscopy (SEM–EDS), and X-ray diffraction (XRD) analyses.

## RESULTS AND DISCUSSION

### Experimental results

#### Flow

Based on the flow results in Figure 6, the highest value was obtained at Na<sub>2</sub>SiO<sub>3</sub>/NaOH ratio of 1:1 with a molarity of 12 M (27%), indicating the best workability. However, a ratio of 2:1 produced the lowest flow at all molarities. For example, 5.41 mm at 10 M showed a thicker and more difficult

to flow mixture. A ratio of 1:1 increased workability, while molarities above 12 M decreased flow due to accelerated geopolymerization reactions. This condition was in line with previous studies, where workability was influenced by Na<sub>2</sub>SiO<sub>3</sub>/NaOH ratio, silicate modulus (SiO<sub>2</sub>/Na<sub>2</sub>O), and liquid/solid ratio. A corresponding increase was observed in viscosity due to rising Na<sub>2</sub>SiO<sub>3</sub>/NaOH ratio, attributed to the formation of silicate oligomers. Meanwhile, excess NaOH levels increased viscosity due to the high ionic strength of alkali solution [19, 20].

#### Initial setting time

The results of Vicat test, the relationship between time and settlement, are shown in Figure 7. Generally, the initial setting time is the duration required for Vicat needle to indicate settlement of 25 mm. Based on the results in Figure 8, M1 and M2 showed longer initial setting time, while M3, M5, and M6 had significantly shorter values. This indicates that increasing the molarity of NaOH accelerates the geopolymerization reaction, leading to a faster setting time, although certain ratios can still slow down the process. Therefore, balanced molarity and activator ratio play an important role in controlling the initial setting. According to previous studies, high alkali concentrations increased the dissolution of silica and alumina, triggering faster polycondensation but shorter setting times [21, 22]. Extremely fast setting time can reduce workability and complicate field applications.

#### Compressive strengt

Figure 9 indicates that the geopolymer’s compressive strength improved with longer curing durations of 3, 7, and 28 days. The highest value of 18.72 MPa was achieved at Na<sub>2</sub>SiO<sub>3</sub>/NaOH ratio of 1:1 on 28 days, with a molarity of 12 M. The 1:1 ratio consistently produced higher compressive strength than 1:2 and 2:1, because the activator balance supported the formation of

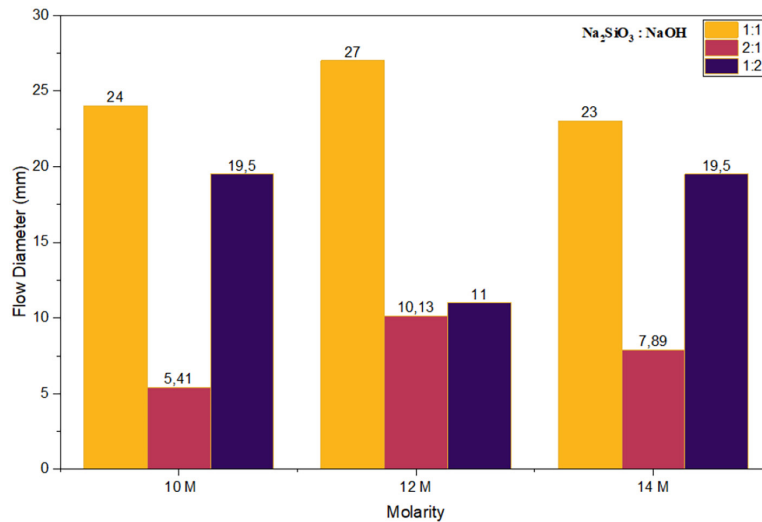


Figure 8. Flow diameter of geopolymer paste

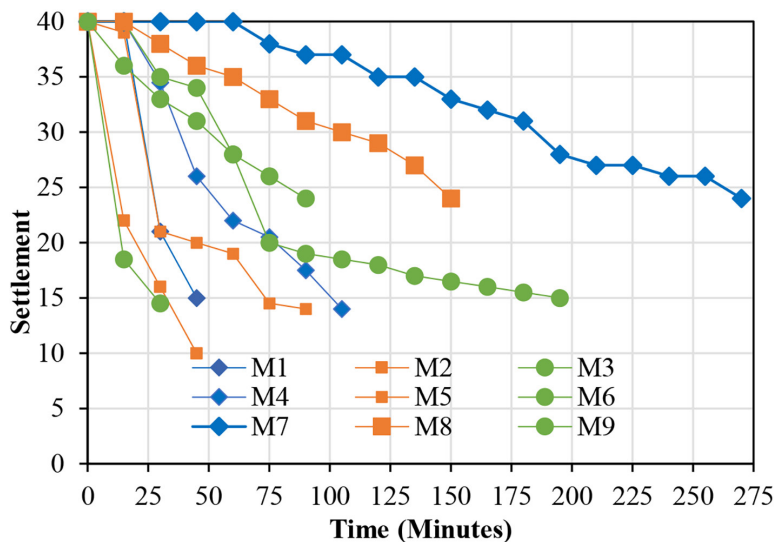


Figure 9. Time and settlement relationship in Vicat test

a dense geopolymer structure. However, the 1:2 ratio often showed the lowest value due to the presence of excess silicate, which inhibited the formation of polymer network. Increasing the molarity from 10 M to 12 M strengthened the structure. There was a slight decrease at 14 M because the reaction was fast, leading to a brittle structure. This result correlated with previous studies on the existence of optimal conditions for the combination of NaOH molarity and  $\text{Na}_2\text{SiO}_3/\text{NaOH}$  ratio. Aluminosilicate dissolution rate was balanced with the silicate supply, leading to the formation of a dense N–A–S–H gel. Extremely high NaOH molarity or fraction can increase porosity and salt precipitation, thereby reducing strength (Figure 11) [30].

### Flexural strength

Flexural strength test results in Figure 10 showed the highest value of 2.4 MPa at a  $\text{Na}_2\text{SiO}_3/\text{NaOH}$  ratio of 1:1 with a molarity of 12 M. Similar to the compressive strength, the 1:1 ratio consistently provided the best performance at all molarities because it produced a more balanced and dense geopolymer bond. The 2:1 ratio produced intermediate results, while 1:2 was consistently the lowest. Furthermore, increasing molarity from 10 M to 12 M showed a corresponding rise in flexural strength, but there was a slight decrease due to extremely rapid reaction at 14 M, causing a more brittle structure. This pattern shows that microstructural densification,

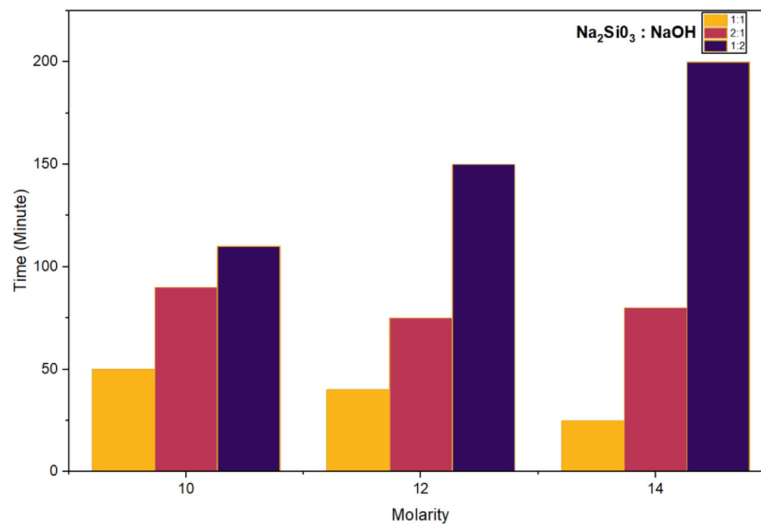


Figure 10. Initial setting time of geopolymer paste

which strengthens the compressive strength, increases the flexural strength. In this study, the optimized geopolymer paste achieved a compressive strength of 18.7 MPa, which is lowest than the 50 MPa reported by [31]. This improvement can be attributed to the formation of a denser and more homogeneous geopolymer gel network, as confirmed by microstructural observations (Figure 12).

### RSM analysis results

#### Input data

The input data for RSM analysis are the experimental results presented in Section 3.1. In this study, there are two factors, including NaOH molarity and Na<sub>2</sub>SiO<sub>3</sub>/total activator ratio, alongside four responses, namely compressive strength, flexural strength, flow, and initial setting time, respectively. The data entered into the Design Expert software for conducting the RSM analysis are presented in Table 3.

#### ANOVA

ANOVA results in Table 4 showed that the models for compressive strength, flexural strength, and initial setting time were significant with a p-value < 0.05. The coefficient of determination (R<sup>2</sup>) was also very high, reaching 1.0, which indicated a good model fit. Although the model for flow was not significant with a p-value of 0.1483 > 0.05, the R<sup>2</sup> value was 0.8651, showing the potential to represent the experimental data. The factors with the most influence on

compressive strength were Na<sub>2</sub>SiO<sub>3</sub>/total activator ratio (B) and the square (B<sup>2</sup>), while NaOH molarity (A), its square (A<sup>2</sup>), and the interaction between the two (AB) showed smaller influence. This is similar for flexural strength, where B and B<sup>2</sup> have a dominant influence, while the other factors are not significant. Although the model is not significant for flow, B and B<sup>2</sup> still show a significant influence on the mixture distribution. At the initial setting time, the most significant influence is from the interaction of AB and B<sup>2</sup> squares, indicating that the interaction between factors plays an important role in determining the setting time. Therefore, Na<sub>2</sub>SiO<sub>3</sub>/total activator is the factor that most consistently affects the mechanical properties of geopolymer.

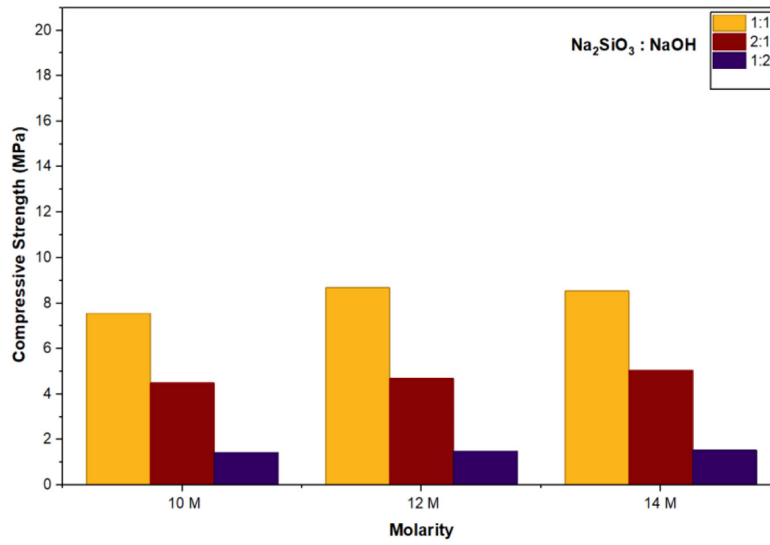
#### Mathematical model

Table 5 shows the coefficients for each item of the selected mathematical model. Based on the statistical analyses reported in earlier studies [30, 32], When the p-value is greater than 0.5, the influence of this item on the response is considered insignificant. The results of the mathematical model of this study are presented in Equations 2–5:

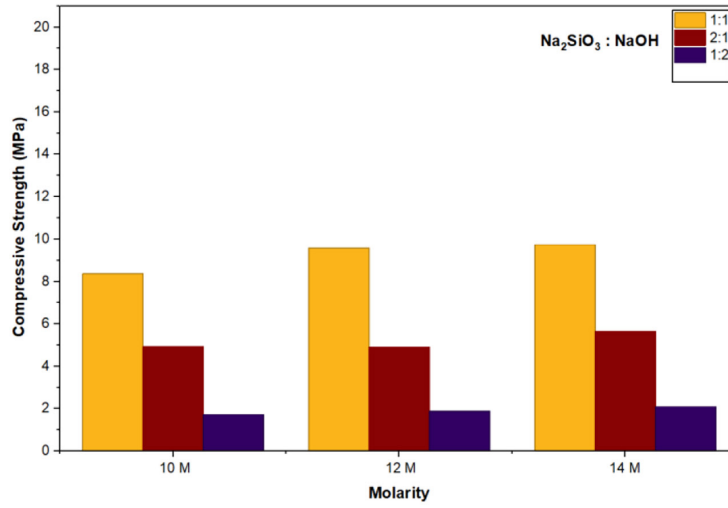
$$f'_c = -105.128 + 0.928A + 4.545B - 0.0138AB - 0.0175A^2 - 0.042B^2 \quad (2)$$

$$f_r = -9.263 - 0.551A + 0.553B - 0.002AB + 0.028A^2 - 0.005B^2 \quad (3)$$

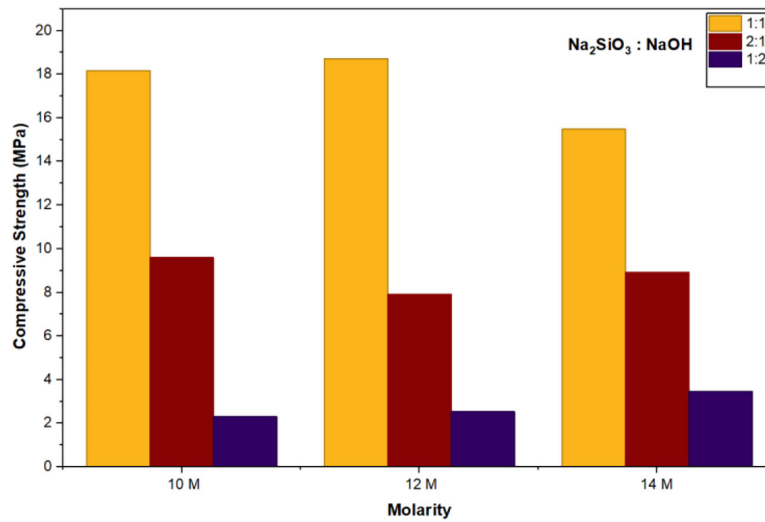
$$r_f = -45.059 - 4.097A + 3.399B + 0.018AB + 0.137A^2 - 0.45B^2 \quad (4)$$



(a)



(b)



(c)

Figure 11. Compressive strength of blended paste at (a) 3 days, (b) 7 days and (c) 28 days

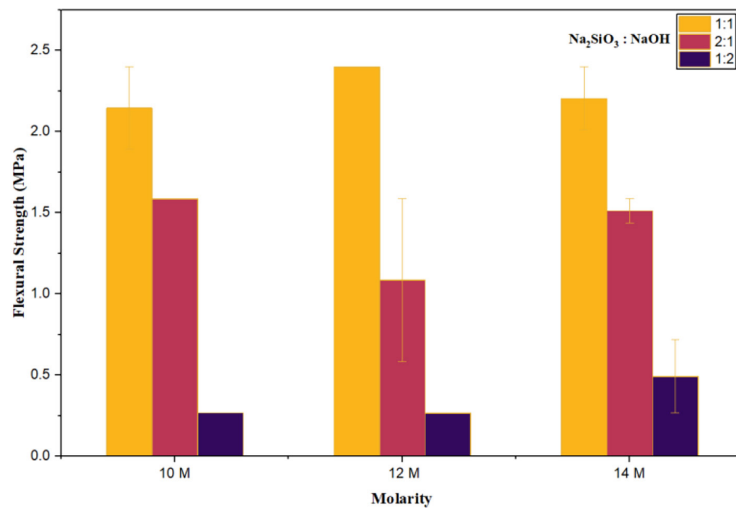


Figure 12. Flexural strengths of blended paste at 28 days

Table 3. Input data into design expert software

Mixtures	NaOH molarity (M)	Na <sub>2</sub> SiO <sub>3</sub> /total activator (%)	Compressive strength (Mpa)	Flexural strength (Mpa)	Flow (%)	Initial setting time (minutes)
M1	10	50	18.17	2.14	24.00	45
M2	12	50	18.72	2.40	27.00	45
M3	14	50	15.49	2.20	23.00	30
M4	10	66.67	9.60	1.59	5.41	270
M5	12	66.67	7.93	1.09	10.13	150
M6	14	66.67	8.93	1.51	7.89	90
M7	10	33.33	2.30	0.27	19.50	105
M8	12	33.33	2.54	0.27	10.87	90
M9	14	33.33	3.47	0.49	19.50	195

$$s_{im} = 831.525 - 72.520 A - 14.090 B - 2.024 AB + 6.875 A^2 + 0.395 B^2 \quad (5)$$

where:  $f'_c$  – compressive strength,  $f_r$  – flexural strength,  $r_f$  – flow, and  $s_{im}$  – initial setting time.

Figure 11 presents RSM results that revealed interaction between the molarity of NaOH solution (A) and the ratio of Na<sub>2</sub>SiO<sub>3</sub> to total activator (B) on the compressive strength of geopolymers paste. The 3D graph showed an optimum peak at a certain combination of variables, where the compressive strength reached a maximum value (18.72 MPa). After passing the optimal condition, increasing the molarity and percentage of Na<sub>2</sub>SiO<sub>3</sub> actually decreased the compressive strength. This phenomenon confirms that increasing the concentration of alkali activator is not often linear with the mechanical strength of the material, but forms a parabolic pattern of increase optimum decrease.

Similarly, previous studies reported that extremely high NaOH molarity could cause the formation of a brittle aluminosilicate gel, thereby reducing strength [18]. In another report, variations in NaOH molarity between 8–12 M were shown to significantly increase the strength in compression of fly ash-based geopolymers. At higher concentrations (14–16 M), the strength decreased due to increased solution viscosity, which inhibited the polycondensation reaction [33, 34].

The ratio of Na<sub>2</sub>SiO<sub>3</sub> to total activator serves a key function in determining the level of polymerization. An extremely high ratio leads to a porous structure with weak bonds, while an optimal ratio allows the formation of a denser and more homogeneous polymer gel network [35, 31]. Therefore, the graphs in this study show that the combination of Na<sub>2</sub>SiO<sub>3</sub> molarity and ratio should be optimized to obtain the best mechanical strength of geopolymers paste material.

**Table 4.** ANOVA results

Responses	Statistical parameters			R <sup>2</sup>	
	Source	F-value	p-value		
Compressive strength (Mpa)	Model	30.34	0.0090	Significant	0.9806
	A	0.3655	0.5881		
	B	25.34	0.0151		
	AB	0.3906	0.5763		
	A <sup>2</sup>	0.0045	0.9506		
	B <sup>2</sup>	125.59	0.0015		
Flexural strength (Mpa)	Model	20.82	0.0155	Significant	0.9720
	A	0.1260	0.7461		
	B	31.45	0.0112		
	AB	0.4252	0.5609		
	A <sup>2</sup>	0.4855	0.5631		
	B <sup>2</sup>	71.63	0.0035		
Flow (%)	Model	3.85	0.1483	Not significant	0.8651
	A	0.0164	0.9063		
	B	5.23	0.1063		
	AB	0.0689	0.8099		
	A <sup>2</sup>	0.0270	0.8800		
	B <sup>2</sup>	13.90	0.0336		
Initial setting time (minutes)	Model	15.84	0.0229	Significant	0.9635
	A	3.02	0.1806		
	B	3.95	0.1412		
	AB	29.96	0.0120		
	A <sup>2</sup>	2.49	0.2129		
	B <sup>2</sup>	39.78	0.0081		

**Table 5.** Mathematical model coefficients described in terms of coded variable

Source	$f'_c$	$f_r$	$r_f$	$s_{tm}$
Intercept	-105.128	-9.263	-45.059	831.525
A	0.928	-0.551	-4.097	-72.520
B	4.545	0.553	3.399	-14.090
AB	-0.0138	- 0.002	0.018	-2.024
A <sup>2</sup>	-0.0175	0.028	0.137	6.875
B <sup>2</sup>	-0.042	- 0.005	- 0.45	0.395

*Multi objective optimization*

Optimization results showed that the use of a low molarity NaOH solution (10 M) provided the most optimal performance. This was indicated by a desirability value of 0.960 compared to other molarities in Table 6. Similarly, previous studies [30] reported that although low molarity could reduce compressive strength by 45–55%, the value was still in the standard range of geopolymer concrete strength. The most suitable

range of Na<sub>2</sub>SiO<sub>3</sub>/total activator ratio was 52.17–53.57%, because outside the value, desirability decreased significantly. This supported previous studies [31, 36]. Which showed an optimal point at alkali concentration, where compressive strength increased by approximately a certain molarity (12–14 M), but decreased at extremely high concentration.

The analysis results showed a significant relationship between flexural and compressive strength, The strong correlation between

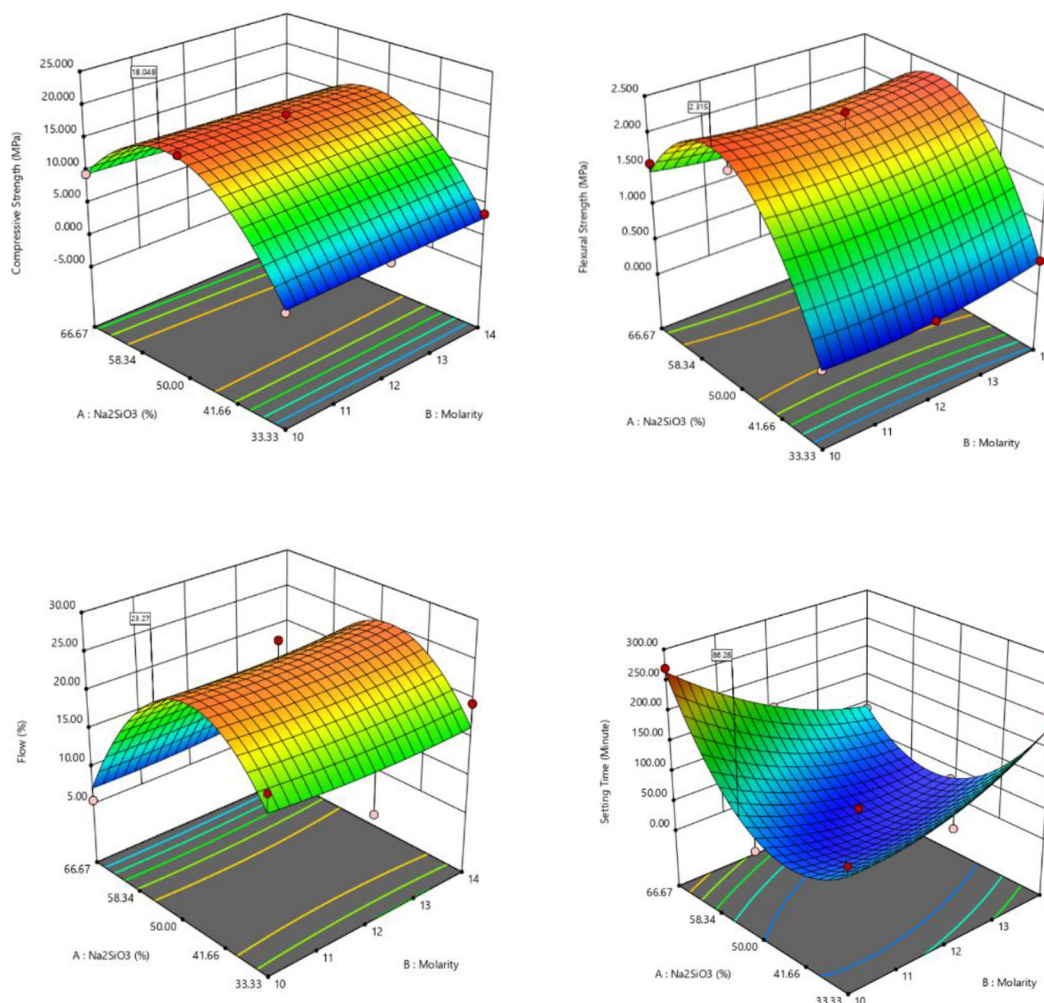


Figure 13. 3D response surfaces: (a) compressive strength; (b) flexural strength; (c) flow; and (d) initial setting time

Table 6. Optimization results

No	NaOH molarity (M)	Na <sub>2</sub> SiO <sub>3</sub> /total activator (%)	$f'_c$ (Mpa)	$f_r$ (Mpa)	$r_f$ (%)	$s_{tm}$ (minutes)	Desirability	Status
1	10.00	53.04	18.048	2.315	23.272	86.283	0.960	In used
2	10.00	53.16	18.042	2.316	23.205	87.175	0.960	-
3	10.00	53.26	18.035	2.316	23.141	88.019	0.959	-
4	10.00	52.71	18.058	2.313	23.457	83.789	0.959	-
5	10.00	53.57	18.012	2.317	22.957	90.428	0.959	-
6	10.00	52.17	18.056	2.306	23.737	79.932	0.958	-
7	14.00	50.64	17.155	2.333	24.932	30.000	0.936	-
8	14.00	56.56	16.278	2.282	21.681	30.000	0.897	-
9	14.00	56.68	16.227	2.278	21.577	30.302	0.894	-
10	13.33	56.71	16.441	2.212	21.083	30.000	0.886	-

compressive and flexural strength observed in Table 6 indicates that improvements in matrix densification and gel continuity simultaneously enhance both load bearing and crack resisting capacities of the geopolymer paste, Under certain

conditions, increasing the molarity of NaOH can improve flexural strength, but decrease compressive strength [31]. Therefore, the best solution is selected in a combination that balances both mechanical parameters. NaOH solutions with

high concentrations tended to accelerate the setting time, reaching the minimum specification limit. This phenomenon was consistent with previous studies [33], where alkali concentration significantly affected the polymerization reaction rate and setting time.

Based on the results of multi objective optimization analysis using RSM, a set of process conditions was identified as the optimal point for the synthesis of geopolymer paste. These conditions were obtained at NaOH molarity of 10 M and a Na<sub>2</sub>SiO<sub>3</sub>/total activator ratio of 53.04%. The results showed that the optimal ratio of Na<sub>2</sub>SiO<sub>3</sub> to NaOH was 53.04:46.96. At this point, the selected model predicts values for all four investigated responses, and the results are presented in Table 7. To validate the accuracy of the developed predictive model, validation experiments were conducted using the optimal parameters, namely a 10 M NaOH solution and a Na<sub>2</sub>SiO<sub>3</sub>:NaOH ratio of 53.04:46.96. The results showed a very high agreement between the predicted and experimental values.

The percentage errors for all responses were below the 5% threshold, which was widely accepted in materials study, showing the validity and reliability of an empirical model [37]. Specifically, the very low errors for flow rate (0.74%) and initial setting time (1.51%) show that the model has excellent predictive ability for the rheological properties and reaction kinetics of geopolymer paste. The low error rates for mechanical properties, namely compressive strength (2.95%) and flexural strength (4.04%), further prove that the developed model is accurate in predicting workability and final structural integrity of geopolymer paste.

### Microstructure

To determine the microstructure of DE based geopolymer, FTIR, SEM, EDS, and XRD tests were carried out on paste under optimal conditions, and the results are described below.

### FTIR

FTIR test results in Figure 12 showed several key absorption bands confirming the formation of sodium aluminosilicate hydrate (N-A-S-H) gel as the main binding phase in the geopolymer paste. The broad band at 3425 cm<sup>-1</sup> showed the presence of O–H groups associated with bound water and hydroxyl in the hydrated gel structure. Meanwhile, the dominant absorption at ~1015 cm<sup>-1</sup> showed the asymmetric Si–O–T (T = Si/Al) stretching, which was characteristic of silicate–aluminosilicate polymerization. It also indicated the formation of Si–O–Al/Si–O–Si framework as the main structure of N-A-S-H gel. An additional band at 864 cm<sup>-1</sup> showed Si–O–Al vibration or silicate ring mode, which confirmed the development of an aluminosilicate oligomer network. The absorption at 1400 cm<sup>-1</sup> and 2274 cm<sup>-1</sup> were related to carbonate due to partial carbonation and possible CO<sub>2</sub> adsorption, respectively, without affecting the identification of the main geopolymer phase. The combination of these bands is overall consistent with N-A-S-H gel formation mechanism in amorphous silica based geopolymer [12].

### SEM-EDS

Figure 13 illustrates the geopolymerization products culminating in the development of N–A–S–H gel from the DE based geopolymer paste, as verified by the EDS analysis. The presence of calcium, alumina, and silica rich diatomaceous earth in the mixture facilitated the formation of sodium aluminosilicate hydrate (N–A–S–H) gel [27]. In this context, DE also contributed additional reactive silica to the system, supporting the development of binding phases and influencing the evolution of the geopolymer gel network. As shown in Figure 12, the detection of Mg<sup>2+</sup> originating from DE suggests the formation of an additional gel phase, characterized as Na–Al(Mg)–Si–H, in agreement with the EDX results. The microcracks observed in several SEM images are likely

**Table 7.** The results of response optimization and those obtained from the validation tests

Responses	Unit	Predicted value	Experimental value	Error (%)
Compressive strength	MPa	18.048	17.53	2.95%
Flexural strength	MPa	2.315	2.225	4.04%
Flow	%	23.27	23.1	0.74%
Setting time	Minutes	86.283	85	1.51%

attributable to the mechanical loading applied during strength testing, since the powders used for SEM analysis were collected from specimens after mechanical failure. In addition, microcracks may have developed due to internal stresses arising between particles during microstructural evolution. This observation is consistent with previous findings, which report that a denser microstructure is closely associated with increased mechanical strength [36].

### XRD pattern

In Figure 14, XRD pattern showed amorphous diffuse agglomerates located around  $27.5^\circ$  ( $2\theta$ ), in the typical range of  $27\text{--}30^\circ$  ( $2\theta$ ), indicating the presence of N-A-S-H gel as the main phase [30, 36]. The silica rich amorphous DE increased the reactivity of the system, thereby accelerating the formation of aluminosilicate network and causing a denser geopolymer matrix with low porosity. The remaining sharp low peaks were likely derived from unreacted quartz or mullite. However, the contribution was minimal and did not detract from the dominant amorphous character of N-A-S-H gel formed in the structure of the geopolymer paste.

## DISCUSSION

The geopolymerization reaction mechanism is characterized by alkaline activation. This is due to mixing of raw materials with alkali solution of the chain, which undergoes polycondensation into a three dimensional gel of N-A-S-H.

At optimum conditions ( $A=10\text{ M}$ ,  $B=53.04\%$   $\text{Na}_2\text{SiO}_3$ ), a balance between dissolution and supply of silicate oligomers is achieved, causing a dense, well bonded gel structure with minimal porosity. This shows an increase in both compressive and flexural strength. However, conditions with excess alkali cause polycondensation to be extremely rapid, higher porosity and reduced long term strength. An increase in NaOH molarity enhanced the compressive and flexural strength up to an optimum level, followed by a reduction at higher molarity due to excessive alkalinity. This behavior is comparable to, which reported an optimum molarity range for dense geopolymer gel formation [37], demonstrated that an unbalanced activator ratio leads to reduced microstructural homogeneity and inferior mechanical performance.

In this study, optimization of DE based geopolymer paste showed that the  $10\text{ M}$  NaOH condition with a  $\text{Na}_2\text{SiO}_3$ /total activator ratio of  $53.04\%$  produced the best mechanical performance with a compressive strength of  $18,048\text{ MPa}$  and a flexural strength of  $2.315\text{ MPa}$ . The improvement was closely related to the microstructural changes occurring at the gel level, as shown by FTIR, SEM EDS, and XRD analyses. The shift of the main Si–O–T ( $T = \text{Si}/\text{Al}$ ) band to a lower wavenumber ( $950\text{ cm}^{-1}$ ) in FTIR showed a rise in Al substitution into the silica framework, indicating a more intensive polycondensation process. Furthermore, the decrease in the intensity of  $-\text{OH}/\text{H}_2\text{O}$  band showed the formation of a more stable gel with a low free water content. SEM images showed a denser matrix with an

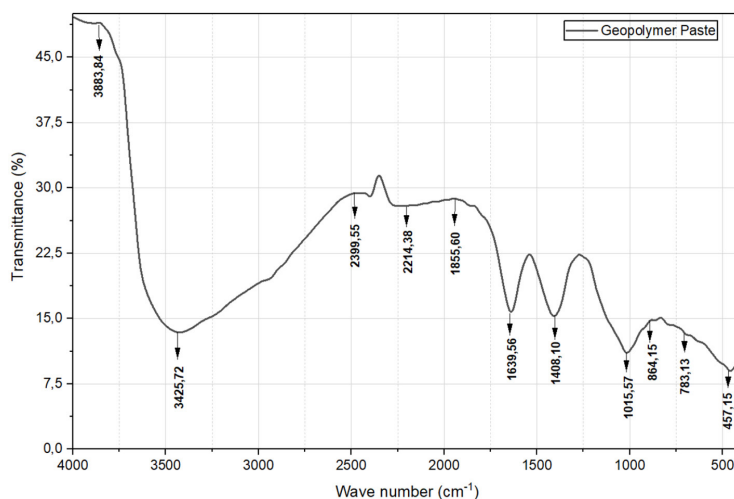


Figure 14. FTIR spectra of the blended geopolymer paste at 28 days

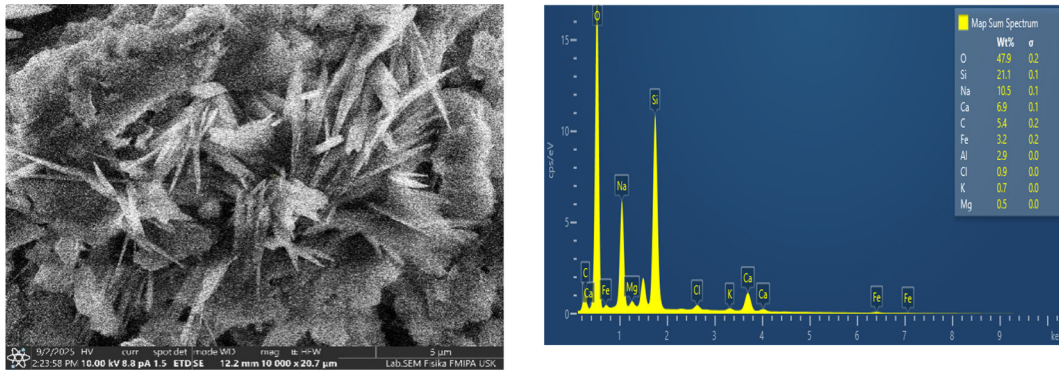


Figure 15. SEM EDS of DE based geopolymer

even gel distribution and minimal number of capillary pores. EDS results showed a homogeneous dominance of Si, Al, Na, and O elements, confirming the formation of an N–A–S–H gel. This is supported by XRD pattern, which shows sharper amorphous protrusions in the range 20–35° 2θ, with a reduction in the quartz crystal peak, indicating the dominance of the amorphous gel phase as the main strengthening factor.

The correlation between microstructural changes and improved mechanical properties is in line with previous results [38]. Another study [32] also showed that controlling NaOH molarity in a moderate range caused a denser microstructure, improving compressive and flexural strength. Additionally, it was observed that optimal NaOH molarity increased the compressive strength and contributed to the flexural strength [15]. This contribution was due to the formation of a homogeneous gel network and good bonding between particles. For DE materials, Tchakouté et al. [13] reported a compressive strength

of approximately 18 MPa at 10 M NaOH and a Na<sub>2</sub>SiO<sub>3</sub>/NaOH ratio of 1.5. However, without optimizing the mixture ratio, the microstructure still showed high porosity. The results indicated that the optimization method used in this study successfully increased gel homogeneity and reduced pores, producing high mechanical properties. During specimen preparation, higher NaOH molarity mixtures exhibited rapid setting and reduced workability. To mitigate these challenges, controlled mixing duration and immediate casting procedures were adopted to ensure homogeneity and minimize premature stiffening.

Zhang et al. [30] reported that increased solution viscosity due to excessively high alkali molarity could hinder the diffusion of silica–alumina ions, leading to a porous structure and reduced strength. A study by Sriram et al. [39] showed that a balanced Na<sub>2</sub>SiO<sub>3</sub>/NaOH ratio played a crucial role in forming a homogeneous matrix with low porosity, improving long term durability. This was supported by Panda et al.

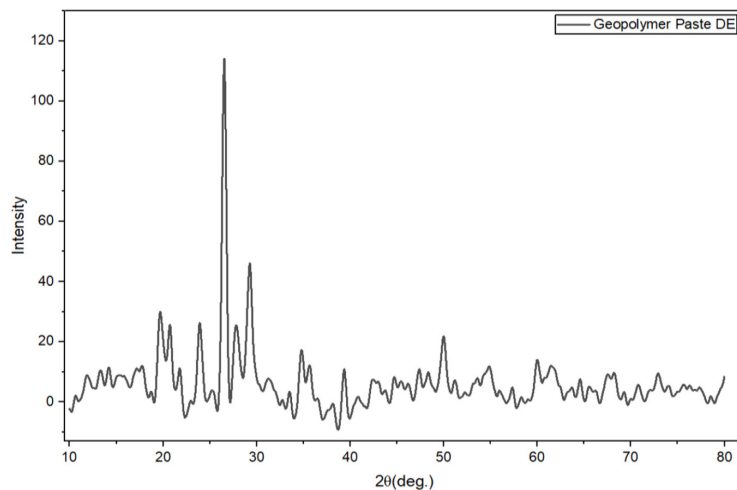


Figure 16. XRD patterns of DE based geopolymer

[36], where low to moderate alkali solutions were found to be capable of producing compressive strengths in the construction standard range, while maintaining the setting time at an acceptable level. Quiatchon et al. used RSM on fly ash based geopolymer paste and emphasized that multi objective optimization obtained the best balance between compressive strength, flexural strength, and setting time.

The increase in compressive and flexural strength at the optimal conditions in this study is a direct consequence of the transformation of the microstructure into a denser, less porous, and richer amorphous phase. The balance between silica–alumina dissolution and silicate oligomer formation achieved at a molarity of 10 M and an appropriate  $\text{Na}_2\text{SiO}_3/\text{NaOH}$  ratio allows the formation of a stable three dimensional N–A–S–H matrix. However, overly alkaline conditions cause excessively rapid polycondensation, leading to gel segregation, high porosity, and low strength. These results are consistent with previous studies [2, 10], where the mechanical properties of geopolymer paste are determined by the chemical composition and evolution of the microstructure during the polymerization process.

## CONCLUSIONS

In summary, the systematic optimization of alkali activator parameters through response surface methodology successfully determined the most effective synthesis conditions for DE based geopolymers. Compared to previous studies, the present research demonstrates superior optimization efficiency through the combined use of molarity and activator ratio variables. However, this study is limited to paste scale investigation; therefore, future work should focus on mortar and concrete level applications, long term durability, and field scale validation. The specimen preparation process revealed several critical practical considerations that influenced the reliability of the experimental results. Maintaining a constant high temperature during furnace treatment was essential to ensure uniform thermal activation of the diatomite, while the rock like hardness of the raw diatomite necessitated a more controlled grinding method than the conventional Los Angeles machine to reduce excessive material loss. Furthermore, the requirement for the ground diatomite to be stabilized at room temperature under air

isolated conditions prior to mixing proved crucial in preserving its physicochemical characteristics, thereby contributing to consistent geopolymerization behavior and reproducible performance outcomes. The optimum composition, consisting of a NaOH concentration of 10 M and a  $\text{Na}_2\text{SiO}_3$  to total activator ratio of 53.04%, produced the highest mechanical performance, with a compressive strength of 18.05 MPa and a flexural strength of 2.32 MPa, while maintaining a deviation of less than 5% between predicted and experimental values. Microstructural investigations using SEM–EDS, XRD, and FTIR revealed that the enhanced strength was associated with the formation of a dense and relatively homogeneous geopolymer matrix, predominantly composed of the N–A–S–H gel composed of  $\text{Na}_2\text{O–Al}_2\text{O}_3\text{–SiO}_2\text{–H}_2\text{O}$  and characterized by low porosity. This matrix was further indicated by an increased amorphous phase and a shift in the Si–O–Si/Al vibration bands. In addition, ANOVA confirmed that the  $\text{Na}_2\text{SiO}_3$  to total activator ratio exerted a more significant influence on the mechanical properties ( $p < 0.05$ ) than the NaOH molarity. Overall, this study establishes an optimized formulation for the utilization of locally available diatomaceous earth as a sustainable geopolymer precursor and provides deeper insight into the interrelationship between processing parameters, microstructural development, and material performance, thereby supporting the advancement of environmentally friendly construction materials.

## Acknowledgements

This study was funded by a doctoral dissertation grant from the Directorate of Research, Technology, and Community Service, Directorate General of Higher Education, Research, and Technology, Ministry of Education, Culture, Research, and Technology of the Republic of Indonesia (contract numbers 614/UN11.2.1/PG.01.03/SPK/DRTPM/2024). The amount of the doctoral dissertation research grant was IDR 37,610,000, and the Head of Research was Prof. Dr. Ir. Taufiq Saidi, M.Eng., IPU.

## REFERENCES

1. Raji Z, Karim A, Karam A, Khalloufi S. Adsorption of heavy metals: mechanisms, kinetics, and applications of various adsorbents in wastewater remediation – A review. *Waste* 2023;1:775–805.

2. Awoyera PO, Adesina A. Plastic wastes to construction products: Status, limitations and future perspective. *Case Stud Constr Mater*. 2020. <https://doi.org/10.1016/j.cscm.2020.e00330>
3. Scrivener KL, John VM, Gartner EM. Eco-efficient cements: Potential economically viable solutions for a low-CO<sub>2</sub> cement-based materials industry. *Cem Concr Res* 2018;114:2–26.
4. Galal Mors HE. Diatomite: Its characterization, modifications and applications. *Asian J Mater Sci* 2010;2:121–136.
5. Al-Ghouti MA, Da'ana DA. Guidelines for the use and interpretation of adsorption isotherm models: A review. *J Hazard Mater* 2020. <https://doi.org/10.1016/j.jhazmat.2020.122383>
6. ElSayed ESEB. Natural diatomite as an effective adsorbent for heavy metals in water and wastewater treatment (a batch study). *Water Sci* 2018;32:32–43.
7. Zhao Y, Tian G, Duan X, Liang X, Meng J, Liang J. Environmental applications of diatomite minerals in removing heavy metals from water. *Ind Eng Chem Res* 2019;58:11638–11652.
8. Cao Y, Ma C, Zhang Q, Shi X, Liu G, Liu X. Hierarchical porous structured SiO<sub>x</sub> derived from diatomite as high performance anode for Li-ion batteries. *J Energy Storage* 2025. <https://doi.org/10.1016/j.est.2025.118141>
9. A R S, Pany C. Static, free vibration and buckling analysis of composite panels; A review. *Adv J Grad Res* 2020;9:21–45.
10. Provis JL, Bernal SA. Geopolymers and related alkali-activated materials. *Annu Rev Mater Res* 2014;44:299–327.
11. Madirisha MM, Dada OR, Ikotun BD. Chemical fundamentals of geopolymers in sustainable construction. *Mater Today Sustain* 2024. <https://doi.org/10.1016/j.mtsust.2024.100842>
12. Kumar M, Rathour R, Singh R, Sun Y, Pandey A, Gnansounou E, Andrew Lin KY, Tsang DCW, Thakur IS. Bacterial polyhydroxyalkanoates: Opportunities, challenges, and prospects. *J Clean Prod* 2020. <https://doi.org/10.1016/j.jclepro.2020.121500>
13. Tchakouté HK, Rüscher CH, Kong S, Kamseu E, Leonelli C. Geopolymer binders from metakaolin using sodium waterglass from waste glass and rice husk ash as alternative activators: A comparative study. *Constr Build Mater* 2016;114:276–289.
14. Enoh MKE, Ushie DO. Effect of sodium silicate to hydroxide ratio and sodium hydroxide concentration on the physico-mechanical properties of geopolymer binders. *East African J Eng* 2023;6:113–121.
15. Abdullah A, Hussin K, Abdullah MMAB, Yahya Z, Sochacki W, Razak RA, Błoch K, Fansuri H. Article the effects of various concentrations of Noah on the inter-particle gelation of a fly ash geopolymer aggregate. *Materials (Basel)* 2021;14:1–11.
16. Smiljanić D, de Gennaro B, Izzo F, Langella A, Daković A, Germinario C, Rottinghaus GE, Spasojević M, Mercurio M. Removal of emerging contaminants from water by zeolite-rich composites: A first approach aiming at diclofenac and ketoprofen. *Microporous Mesoporous Mater* 2020. <https://doi.org/10.1016/j.micromeso.2020.110057>
17. Ibrahim S, ElBatal FH, Abdelghany AM. Optical character enrichment of NdF<sub>3</sub> – doped lithium fluoroborate glasses. *J Non Cryst Solids* 2016;453:16–22.
18. IDas D, Rout PK. Effect of NaOH concentration on the mechanical and microstructural properties of fly ash-based geopolymer. *Biointerface Res Appl Chem* 2025. <https://doi.org/10.33263/BRIAC151.013>
19. Shi X, Zhang C, Wang X, Zhang T, Wang Q. Response surface methodology for multi-objective optimization of fly ash-GGBS based geopolymer mortar. *Constr Build Mater* 2022. <https://doi.org/10.1016/j.conbuildmat.2021.125644>
20. Quiatchon PRJ, Dollente IJR, Abulencia AB, De Guzman Libre RG, Villoria MBD, Guades EJ, Promentilla MAB, Ongpeng JMC. Investigation on the compressive strength and time of setting of low-calcium fly ash geopolymer paste using response surface methodology. *Polymers (Basel)* 2021. <https://doi.org/10.3390/polym13203461>
21. Yahya Z, Abdullah MMAB, Hussin K, Ismail KN, Razak RA, Sandu AV. Effect of solids-to-liquids, Na<sub>2</sub>SiO<sub>3</sub>-to-NaOH and curing temperature on the palm oil boiler ash (Si + Ca) geopolymerisation system. *Materials (Basel)* 2015;8:2227–2242.
22. Hasan M, Saidi T, Mubarak A, Jamil M. Effect of calcined diatomaceous earth, polypropylene fiber, and glass fiber on the mechanical properties of ultra-high-performance fiber-reinforced concrete. *J Mech Behav Mater* 2023. <https://doi.org/10.1515/jmbm-2022-0275>
23. Hayati S, Muttaqin M, Saidi T. Studi kuat tekan dan kuat lentur pasta semen campuran dengan tanah diatomae. *J Civ Eng Student* 2020;2:127–133.
24. ASTM C1437. Standard, A., C1437. *Astm C* 2009;1437:15–16.
25. ASTM C-08. Standard test methods for time of setting of hydraulic cement by Vicat needle. *ASTM Int* 2014;8:3–4.
26. ASTM C109/109M. Standard test method for compressive strength of hydraulic cement mortars (Using 2-in. or cube specimens). *Annu B ASTM Stand* 2016;1–10.
27. American Society for Testing and Materials. C78-02. Standard Test Method for Flexural Strength of Concrete. *Am Soc Test Mater* 2002;1–3.

28. Ba D, Boyaci IH. Modeling and optimization i: Usability of response surface methodology. *J Food Eng* 2007;78:836–845.
29. Deb K, Pratap A, Agarwal S, Meyarivan T. A fast and elitist multiobjective genetic algorithm: NSGA-II. *IEEE Trans Evol Comput* 2002;6:182–197.
30. Zhang P, Gao Z, Wang J, Guo J, Hu S, Ling Y. Properties of fresh and hardened fly ash/slag based geopolymer concrete: A review. *J Clean Prod* 2020. <https://doi.org/10.1016/j.jclepro.2020.122389>
31. Saha S, Rajasekaran C. Enhancement of the properties of fly ash based geopolymer paste by incorporating ground granulated blast furnace slag. *Constr Build Mater* 2017;146:615–620.
32. Li Z, Lu D, Gao X. Optimization of mixture proportions by statistical experimental design using response surface method – A review. *J Build Eng* 2021. <https://doi.org/10.1016/j.jobbe.2020.102101>
33. Sunarsih ES, As'ad S, Mohd. Sam AR, Kristiawan SA. The effect of sodium hydroxide molarity on setting time, workability, and compressive strength of fly ash-slag-based geopolymer mortar. *J Phys Conf Ser* 2023. <https://doi.org/10.1088/1742-6596/2556/1/012019>
34. Qin TS, Lim NHAS, Jun TZ, Ariffin NF. Effect of low molarity alkaline solution on the compressive strength of fly ash based geopolymer concrete. *Int J Sustain Build Technol Urban Dev* 2022;13:155–164.
35. Lee M, Tsai WS, Chen ST. Reusing shell waste as a soil conditioner alternative? A comparative study of eggshell and oyster shell using a life cycle assessment approach. *J Clean Prod* 2020. <https://doi.org/10.1016/j.jclepro.2020.121845>
36. Panda B, Unluer C, Tan MJ. Investigation of the rheology and strength of geopolymer mixtures for extrusion-based 3D printing. *Cem Concr Compos* 2018;94:307–314.
37. Lee WKW, Van Deventer JSJ. The effect of ionic contaminants on the early-age properties of alkali-activated fly ash-based cements. *Cem Concr Res* 2002;32:577–584.
38. Duxson P, Van Deventer JSJ. Commercialization of geopolymers for construction - opportunities and obstacles. *Geopolymers Struct Process Prop Ind Appl* 2009;379–400.
39. Sriram G, Kigga M, Uthappa UT, Rego RM, Thendral V, Kumeria T, Jung HY, Kurkuri MD. Naturally available diatomite and their surface modification for the removal of hazardous dye and metal ions: A review. *Adv Colloid Interface Sci* 2020. <https://doi.org/10.1016/j.cis.2020.102198>